# I/Q Imbalance and CFO in OFDM/OQAM Systems: Interference Analysis and Compensation

Aamir Ishaque and Gerd Ascheid
*Institute for Communication Technologies and Embedded Systems, RWTH Aachen University, Germany
Email: {ishaque,ascheid}@ice.rwth-aachen.de

***Abstract*—Offset-QAM (OQAM) based OFDM has been considered as a promising technique for future wireless networks due to its higher resilience to narrow-band interference and doubly dispersive channels. In this paper, we investigate the effects of the RX imperfections, namely the I/Q imbalance (IQI) and the carrier frequency offset (CFO), on OFDM/OQAM downlink performance coupled with the imperfect knowledge of the frequency-selective channel. The influence of each impairment is characterized by the interference analysis of the demodulated signal that reveals interesting insight into the distortion origination. Then, we analytically investigate the performance loss as a function of IQI, CFO and channel distortions in a realistic receiver with channel estimation error. To cope with impaired reception, a joint maximum-likelihood estimation method with repetitive training signals is employed. Simulation results demonstrate the relative sensitivity of OFDM/OQAM receivers to the impairments and that the performance loss due to the imperfections can be recovered by the compensation technique.**

## I. Introduction

Multicarrier transmission is a widely adopted modulation technique for communication over time-dispersive channels. In orthogonal frequency division multiplexing (OFDM), a cyclic signal extension (CP) helps maintain orthogonality of subcarriers and reduces the complexity of multipath channel equalization task by evading intersymbol (ISI) and intercarrier (ICI) interference. While a conservative selection of the guard period in a dynamic channel environment causes a waste of spectral resources and the elevation of the power budget, a modest design would inevitably result in the loss of orthogonality. Moreover, a rectangular pulse shape in OFDM/QAM system implies a gentle side-lobe decay and a high ICI level due to frequency dispersion and synchronization loss. A basic design principle has been to search for pulse shapes that are well-localized both in time and frequency to limit energy spilling to the neighboring lattice points [1]. However, the Ballin-Low theorem prohibits the existence of Gabor frames well-concentrated in time and frequency when operating at critical spectral density [2, and references therein]. Therefore, the optimum pulse shapes in OFDM/QAM systems have been restricted to Weyl-Heisenberg frames employing non-(bi)orthogonal designs [3]. For that case, under-critical Riesz basis requires sacrificing the spectral efficiency [1], unless higher-order equalizers are targeted [4].

OFDM systems based on offset-QAM (OQAM) have been proposed in 3GPP-LTE standard [5] as a promising technique to alleviate drawbacks of the conventional OFDM/QAM transmultiplexers by adopting a filter-bank multicarrier (FBMC) transmission paradigm [6]. Restricting the orthogonality constraint to real fields, it allows non-rectangular pulse shape with minimal bandwidth and fixed temporal support at the expense of increased complexity due to symbol overlap and a prolonged interference pattern in highly dispersive channels [2]. Nevertheless, this flexibility allows prototype filter design with different objectives in mind e.g., preshaping in accordance with the ISI/ICI helps combat the channel dispersion [4] or the carrier frequency-offset (CFO) induced perturbation [7].

So far, an in-depth understanding of OFDM/OQAM operation with practical receivers (i.e., suffering from inevitable RF imperfections and channel estimation inaccuracy) has been largely overlooked in literature. It seems that this problem has only been studied from the perspective of synchronization errors in [2], [8]. In [7], signal-to-noise ratio (SNR) degradation was investigated in the presence of CFO over flat fading channels and it was shown that FBMC/OQAM is less sensitive to CFO than OFDM/QAM. The effect of CFO with multi-path propagation was studied in [9], where performance convergence to non-dispersive channels was observed for systems with large number of subcarriers. However, the influence of additive noise and channel estimation error on fading equalization were entirely ignored. Direct-conversion receivers (DCRs) have received a lot of attention over the past two decades favored by their integration capability and low cost. However, the practical implementation of DCR suffers from several problems due to manufacturing inaccuracies raising issues, particularly I/Q imbalance (IQI). There exists abundant literature on mitigating critical impairments in OFDM/QAM systems (e.g., [10], [11]).

In this article, we study the robustness of OFDM/OQAM systems to RF impairments; IQI and CFO, given the imperfect channel knowledge. Through our formulation, it will be revealed that the impairment characterization differs considerably from OFDM/QAM and is uniquely determined by the prototype filter design. To maintain and realize reliable communication with RF distortion, we present an OFDM/OQAM-based system that maintains a certain degree of compatibility with the conventional OFDM specification. Specifically, we aim to estimate IQI and CFO in a maximum-likelihood (ML) data-aided technique that operates over two identical preamble sequences, followed by time-domain estimation of the channel impulse response (CIR) using channel training block. However, compared to [8], the preamble overhead for CFO estimation is reduced by discarding the *transition period*. Numerical experiments are presented to analyze the relative sensitivity of OFDM/OQAM systems to imperfections and assess BER improvement, when utilizing the compensation method.

*Notation*: $(\cdot)^*$, $(\cdot)^T$, $(\cdot)^H$, $(\cdot)^\dagger$ and $(\cdot)_N$ denote conjugation, transpose, conjugate transpose, pseudo-inverse and modulo-$N$ operations respectively; $\mathbf{I}$ and $\mathbf{0}$ represents the identity matrix

*Part of this work has been performed in the framework of the FP7 project ICT-317669 METIS, which is partly funded by the European Union. The authors would like to acknowledge the contributions of their colleagues in METIS, although the views expressed are those of the authors and do not necessarily represent the project.

and the null matrices respectively; $[\cdot]_{m,n}$ provides the $(m,n)$-th element of the argument matrix; $\mathrm{Tr}\{\cdot\}$, $\mathbb{E}\{\cdot\}$, $\Re\{\cdot\}$ and $\Im\{\cdot\}$ refer to trace, expectation, real and imaginary operators respectively; $\jmath = \sqrt{-1}$; $\odot$ and $\otimes$ represent element-wise multiplication and convolution respectively.

## II. OFDM/OQAM System With Imperfections

We consider an OFDM/OQAM system with $K$ subcarriers that are modulated by data symbols $\boldsymbol{s}_{\bar{n}} \in \mathbb{C}^{K\times 1}$ taken out of a QAM constellation, and assumed to be independent and identically distributed (i.i.d.) with zero mean and variance $\sigma_s^2$. The real $s^I_{\bar{n},m}$ and imaginary $s^Q_{\bar{n},m}$ part of the complex symbols $s_{\bar{n},m}$ are transmitted on pulses staggered by $T/2$ and the adjacent subcarriers are staggered oppositely. The sampled multicarrier signal at the rate $T_s = T/K$ is equal to

$$u(k) = \sum_{n=\lceil \frac{k+1}{M} \rceil - \tau}^{\lfloor \frac{k}{M} \rfloor + \tau} \sum_{m=0}^{K-1} g\left(k - nM\right) a_{n,m} \times \exp\left(\jmath \frac{2\pi}{K} m\left(k-\varrho\right)\right) \exp\left(\jmath \varphi_{n,m}\right) \quad (1)$$

where $K = 2M$, $a_{n,m} \in \{s^I_{\bar{n},m}, s^Q_{\bar{n},m}\}$, $n \in \{2\bar{n}, 2\bar{n}+1\}$ and $\tilde{g}(k) = g(k - L/2)$ is the real-valued prototype filter with unit energy and time-limited to $[0\ LT_s)$. For an integer-length filter $g(k)$ i.e., $L = \tau K \in \mathbb{Z}^+$, the pulse phase factor corresponds to $\varrho = (L-1)/2$ [2], whereas the subcarrier phase factor was assumed as $\varphi_{n,m} = (\pi(n+m)/2)_\pi$ in [6]. Let $\zeta_{n,m}(k)$ be the synthesis function which is offset in time by $n$ and in frequency by $m$, then (1) becomes,

$$u(k) = \sum_{n=\lceil \frac{k+1}{M} \rceil - \tau}^{\lfloor \frac{k}{M} \rfloor + \tau} \sum_{m=0}^{K-1} \zeta_{n,m}(k) a_{n,m}. \quad (2)$$

The baseband signal undergoes digital-analogue conversion and then up-converted after low-pass filtering through $\Psi_T(t)$ to remove higher-order components. The transmitted signal passes through a propagation channel channel characterized by the impulse response $h_T(t) = \Psi_T(t) \otimes h_{BB}(t)$. The complex additive baseband noise $w(t)|_{t=kT_s}$ is assumed to be i.i.d. and have proper Gaussian distribution with zero mean and variance $\sigma_w^2$. The bandpass signal at the RX mixing stage can be represented by

$$r_{\mathrm{RF}}(t) \triangleq \sqrt{2}\Re\left\{x(t) e^{\jmath w_c t}\right\} \quad (3)$$

where $x(t) = v(t) + w(t)$ is the baseband signal and $v(t) = u(t) \otimes h_T(t)$. The output of the local oscillator is expressed as

$$d(t) \triangleq \cos\left(w_c t + \Delta w t\right) + \jmath\left(1+\varepsilon\right)\sin\left(w_c t + \Delta w t + \theta\right) \quad (4)$$

where $\varepsilon$ and $\theta$ denote the amplitude and phase mismatch respectively, and $\Delta w = 2\pi\Delta f$ is the angular frequency offset. The received RF signal $r_{\mathrm{RF}}(t)$ is downconverted to baseband signal $r(t)$ by DCR method and a low-pass filter $\Psi_R(t)$ is applied to remove high-frequency components. Sampling $r(t)$ at the rate $T_s$ results in a discrete-time baseband signal,

$$r(k) = \alpha e^{-\jmath \Delta w k T_s} x(kT_s) + \beta e^{\jmath \Delta w k T_s} x^*(kT_s) \quad (5)$$

in which $\alpha \triangleq \left(1 + (1+\varepsilon)\, e^{-\jmath\theta}\right)/2$ and $\beta \triangleq \left(1 - (1+\varepsilon)\, e^{\jmath\theta}\right)/2$. At the demodulator stage, the received signal $y_{n',m'}$ located on $n'$-th time index and $m'$-th frequency index is obtained by projecting $r(k)$ on to the matched filter function $\zeta^*_{n',m'}$ as

$$y_{n',m'} = \langle r, \zeta^*_{n',m'} \rangle \triangleq \sum_{k\in\mathbb{Z}} \zeta^*_{n',m'}(k) r(k) \quad (6)$$

and taking the real part of the linear one-tap equalized signal, we get the symbol estimate as

$$\hat{a}_{n',m'} = \Re\left\{\frac{y_{n',m'}}{H(m')}\right\} \quad (7)$$

where $H(m)$ is the discrete Fourier transform of the effective zero-mean and sample-spaced CIR $h(n) = \Psi_T(t) \otimes h_{BB}(t) \otimes \Psi_R(t)|_{t=nT_s},\ \forall\ 0 \le n < L_g$.

### A. Channel Fading

The demodulated signal with the time-dispersive channel and ideal RF processing is formulated in Appendix A. From (32), it is clear that the orthogonality amongst the subcarriers is destroyed by the channel time-dispersion. Each subcarrier undergoes flat fading and additionally suffers from *intrinsic interference* as a consequence of the purely-imaginary ambiguity function $A_g(\Delta n, \Delta m)$ in the odd-ordered neighborhood $\Omega''$. Note that the cancellation of the intrinsic interference depends on the channel spectral-correlation and the OFDM/OQAM principle. For low correlation regime or high frequency-selectivity, the residual interference can be substantial. This problem has been circumvented by using higher-order equalizers or by introducing CP in a redundant OFDM/OQAM system [12] (beyond the scope of this article). Due to the decaying nature of the ambiguity function $A_g(\Delta n, \Delta m)$, the time-frequency lattice map $\Omega$ of the interference pattern has potentially a lower-order neighborhood in time $\Omega^{(t)}$ and frequency $\Omega^{(f)}$, restricting interference analysis to $\bar{\Omega} = \left(\Omega^{(t)}, \Omega^{(f)}\right)$.

### B. IQI distortion

When the channel is non-dispersive and IQI distorts the received signal $\hat{a}_{n',m'}$, the unconjugated filter term causes interference $\mathcal{I}^{uc}$ from the desired subcarrier neighborhood, while the conjugated counterpart causes interference $\mathcal{I}^{c}$ from the mirror subcarrier and its neighborhood. If the desired and image subcarriers are well-separated, the interference patterns do not overlap i.e., $\left(n' - \Omega^{(t)}\right) \times \left(m' - \Omega^{(f)} \cap \Omega^{(f)} - m'\right) = \emptyset$, and $\mathcal{I}_c$ is statistically independent of $\mathcal{I}_{uc}$ . For any arbitrary $(n', m')$-th symbol point, the interference composition is

$$\mathcal{I}^{uc}_{n',m'} = \sum_{\substack{(\Delta n,\Delta m)\in\bar{\Omega} \\ (\Delta n,\Delta m)\neq(0,0)}} J_\alpha\left(\Delta n, \Delta m\right) A^{\pm}_g(\Delta n, \Delta m) a_{n,m} \quad (8)$$

$$\mathcal{I}^{c}_{n',m'} = \sum_{(\Delta n,\Delta m)\in\bar{\Omega}} J_\beta\left(\Delta n, \Delta m\right) A^{\pm}_g(\Delta n, \Delta m) a_{n,-m} \quad (9)$$

where $A^{\pm}_g(\Delta n, \Delta m) = \pm A_g(\Delta n, \Delta m)$, the symbol point $a_{n,-m}$ lies at the frequency mirror-image location of $a_{n,m}$,

$$J_\alpha(\Delta n, \Delta m) = \begin{cases} \Re\{\alpha\} & (\Delta n, \Delta m) \in \Omega' \\ -\Im\{\alpha\} & \text{Otherwise,} \end{cases} \quad (10)$$

and similarly follows $J_\beta(\Delta n, \Delta m)$.

*Remarks*

1) From (8) and (9), it is clear that the total interference power $\mathrm{I}_{IQI}^{OQAM}$ affecting $\boldsymbol{s}_{\bar{n}}$ is independent of $\bar{n}$ and

$$\mathrm{I}_{IQI}^{OQAM} = 2\mathbb{E}_{\boldsymbol{a}}\left\{|\mathcal{I}^{uc}|^2 + |\mathcal{I}^{c}|^2\right\} \quad (11)$$

$$\geq \mathrm{I}_{IQI}^{QAM} = |\beta|^2\sigma_s^2 \quad (12)$$

which implies higher IQI sensitivity of the OFDM/OQAM system. The equality holds either for $\alpha, \beta \in \mathbb{R}$ or when $A_g(\Delta n, \Delta m) \to 0 \; \forall \; (\Delta n, \Delta m) \in \Omega'' = \Omega \backslash \Omega'$. The former happens for a small degree of phase mismatch i.e., $\theta \to 0$ whereas the later proposition is a pessimistic condition because non-zero $A_g(\Delta n, \Delta m)$ in the desired subcarrier neighborhood $\Omega''$ plays a crucial role in time/frequency localization properties [13].

2) Due to the interplay between (8) and (9), $\mathcal{I}^{c}_{n',m'}$ cannot be shaped separately from $\mathcal{I}^{uc}_{n',m'}$. Hence, a significant minimization of $\mathrm{I}_{IQI}^{OQAM}$ by optimizing over $g(n)$ is difficult to achieve. Even when possible, the inequality in remark 1 cannot be violated.

3) The presence of IQI in the demodulated signal leads to ISI, ICI and interference amongst the real and imaginary parts of the complex data symbols $s_{\bar{n},m}$.

4) The variance of the effective additive noise terms in (6) is a function of IQI parameters and is given, for any arbitrary $n'$, as $\sigma^2_{\tilde{w}} = \left(|\alpha|^2 + |\beta|^2\right)\sigma^2_w/2$. This relation holds for the normalized pulse shapes i.e., $\sum_{n=0}^{L-1}|g(n)|^2 = 1$ that satisfy orthogonal condition $\sum_{k\in\mathbb{Z}}\zeta^*_{n',m'}(k)\zeta_{n,m}(k) = \delta_{\Delta n,\Delta m}$, where $\delta_{n,m}$ is the Kronecker delta function.

### C. CFO distortion

Consider the symbol estimate $\hat{a}_{n',m'}$ perturbed by the normalized CFO $\overline{\Delta f} = \Delta f K T_s$. The accumulated interference at the output of the $(n',m')$-th analysis filter-bank is given by

$$\mathcal{I}^{\Delta f}_{n',m'} = \sum_{\substack{(\Delta n,\Delta m)\in\bar{\Omega}'\\(\Delta n,\Delta m)\neq(0,0)}} \Re\left\{e^{-\jmath\frac{\pi}{2}(n+n')\overline{\Delta f}}A_g^{\pm}(\Delta n, \Delta m + \overline{\Delta f})\right\}a_{n,m}$$

$$- \sum_{(\Delta n,\Delta m)\in\bar{\Omega}''} \Im\left\{e^{-\jmath\frac{\pi}{2}(n+n')\overline{\Delta f}}A_g^{\pm}(\Delta n, \Delta m + \overline{\Delta f})\right\}a_{n,m} \quad (13)$$

where $\bar{\Omega}' = \bar{\Omega}\cap\Omega'$, $\bar{\Omega}'' = \bar{\Omega}\cap\Omega''$ and $A_g(\Delta n, \Delta m + \overline{\Delta f})$ is no longer a real-valued function.

*Remarks*

1) From (13), we note that the frequency offset $\overline{\Delta f}$ causes a modulation phase drift $\Phi_n = e^{-\jmath\frac{\pi}{2}n\overline{\Delta f}}$ from the symbol blocks in the neighborhood $\Delta n \in \Omega^{(t)}$, an attenuation $A_g(0, \overline{\Delta f})$ of the useful signal coming from the power leakage to the neighboring subcarriers, and the interference terms from neighboring lattice points characterized by the frequency-shifted ambiguity function i.e., $A_g(\Delta n, \Delta m + \overline{\Delta f})$.

2) The common phase error (CPE) term $\mathcal{K}^{\Delta f}_{\mathrm{CPE}} = \exp\left(-\jmath\pi\overline{\Delta f}n'/2\right)A_g(0, \overline{\Delta f})$ causes a periodic variation in degradation over the symbol blocks $n'$. When a pilot-assisted channel estimation is employed, CPE is assimilated into the channel estimates and inherently suppressed by the channel equalizer.

3) A rapid spectral decay of $g(n)$ to reduce ISI/ICI due to CFO is always feasible[1] and hence, $\mathrm{I}_{CFO}^{OQAM} \leq \mathrm{I}_{CFO}^{QAM}$ is achieved by most of the frequency-localized filters. In fact, the rectangular pulse, which theoretically has similar error performance as OFDM/QAM systems in AWGN channels, serves as the worst case.

## III. Influence on Coherent Reception

The benefits of OFDM/OQAM come at the cost of relaxation of the orthogonality condition to real fields. As mentioned earlier, the intrinsic interference between the neighboring subcarriers distorts the inter-subcarrier relationship. Therefore, a meaningful metric depicting the influence of impairments in fading channels should be stated using equalized symbols $\hat{\boldsymbol{a}}_{n'}$. We measure the imperfectness of the reception by calculating the signal-to-interference-plus-noise ratio (SINR) degradation:

$$\mathrm{D} = 10\log 10\left\{\frac{\mathrm{SINR}_{\mathrm{Ideal}}}{\mathrm{SINR}_{\mathrm{Imp}}}\right\} \quad (14)$$

defined as the difference in dB between the received SINRs of the ideal and impaired receivers. Switching to matrix notation, exploiting (32), and considering IQI (8)-(9) and CFO (13), we can rewrite the transmission equation (6) as

$$\boldsymbol{y}_{n'} = \sum_{n=-\tau+1}^{\tau}\Big(\underbrace{\alpha e^{-\jmath\frac{\pi}{2}(n+n')\overline{\Delta f}}\tilde{\mathbf{H}}\odot\tilde{\mathbf{G}}_n}_{=:\,\boldsymbol{\Upsilon}^{\alpha}_{n',n}}$$

$$+\underbrace{\beta e^{\jmath\frac{\pi}{2}(n+n')\overline{\Delta f}}\bar{\mathbf{H}}\odot\bar{\mathbf{G}}_n}_{=:\,\boldsymbol{\Upsilon}^{\beta}_{n',n}}\Big)\boldsymbol{a}_{n'+n}$$

$$+\alpha\sum_{n=-\tau+1}^{\tau}\mathbf{F}_n^H\boldsymbol{w}_{n'+n} + \beta\sum_{n=-\tau+1}^{\tau}\mathbf{F}_n^H\boldsymbol{w}^*_{n'+n} \quad (15)$$

where $\boldsymbol{y}_{n'} = [y_{n',0}, y_{n',1}, \ldots, y_{n',K-1}]^T$, $\boldsymbol{a}_{n'} = [a_{n',0}, a_{n',1}, \ldots, a_{n',K-1}]^T$, $\boldsymbol{w}_{n'} = [w_{n',0}, w_{n',1}, \ldots, w_{n',M-1}]^T$, $[\tilde{\mathbf{H}}]_{m',m} = H\big((m+m')_K/2\big)$, $[\bar{\mathbf{H}}]_{m',m} = H^*\big((m-m')_K/2\big)$, $[\mathbf{F}_n]_{k,m} = \zeta_{n,m}(k)$ is a $M\times K$ synthesis matrix, $[\tilde{\mathbf{G}}_n]_{m',m} = A_g(\Delta n, \Delta m + \overline{\Delta f})\exp\left(\jmath\tilde{\theta}_{\Delta n,\Delta m}\right)$, $\left[\bar{\mathbf{G}}_n\right]_{m',m} = A_g(\Delta n, \overline{\Delta m} - \overline{\Delta f})\exp\left(\jmath\tilde{\theta}_{\Delta n,\overline{\Delta m}}\right)$ and $\overline{\Delta m} = m' + m$. Note that in the absence of CFO, we have $K\times K$ I/O filter-bank matrix as $\tilde{\mathbf{G}}_n|_{\Delta f=0} = \sum_l \mathbf{F}_l^H\mathbf{F}_{l+n}$. The channel fading in (15) is inverted by a one-tap zero-forcing equalizer (ZFE): $\mathbf{Z} = \hat{\mathbf{H}}^{-1}$. Unaware of non-idealities, the channel estimator is prone to channel estimation error (CEE) modeled by an additive error matrix $\boldsymbol{\Delta}_H$ and a scaling ambiguity $\tilde{\alpha} = \alpha\mathcal{K}^{\Delta f}_{\mathrm{CPE}}$, so that

$$\hat{\mathbf{H}} = \tilde{\alpha}\mathbf{H} + \boldsymbol{\Delta}_H \quad (16)$$

where the error term is assumed to be proper Gaussian with $\boldsymbol{\Delta}_H \sim \mathcal{CN}(\mathbf{0}, \mathbf{C}_{\boldsymbol{\Delta H}})$. In practice, the channel estimates $\hat{\mathbf{H}}$ are usually obtained by time-domain least-squares method, which is identical to ML criterion with linear Gaussian model and is known to achieve Cramér-Rao bound. Defining $\mathbf{U}_{n'}$ as a $M - L_g \times L_g$ truncated Toeplitz matrix constituted by the time-domain training sequence $\boldsymbol{u}_{n'}$ in $n'$-th symbol, the diagonal CFO matrix $[\mathbf{E}_{n'}]_{k,k} = \exp\left(-\jmath 2\pi(k + n'M + L_g)\overline{\Delta f}/K\right)$

[1] One approach is to displace the spectral nulls of $g(n)$ by the expected value of the normalized CFO $\overline{\Delta f}$ [7].

and $\mathbf{C}_{\boldsymbol{h}} = \mathbb{E}\left\{\boldsymbol{h}\boldsymbol{h}^H\right\}$, the CEE covariance matrix for the channel estimates $\hat{\boldsymbol{h}} = [\hat{h}_0, \hat{h}_1, \ldots, \hat{h}_{L_g-1}]^T$ is given by

$$\begin{aligned}\mathbf{C}_{\boldsymbol{\Delta h}} &= \mathbb{E}\left\{\left(\hat{\boldsymbol{h}} - \tilde{\alpha}\boldsymbol{h}\right)\left(\hat{\boldsymbol{h}} - \tilde{\alpha}\boldsymbol{h}\right)^H\right\} \qquad (17)\\ &= \left(\alpha\mathbf{U}_{n'}^{\dagger}\mathbf{E}_{n'}\mathbf{U}_{n'} - \tilde{\alpha}\mathbf{I}\right)\mathbf{C}_{\boldsymbol{h}}\left(\alpha\mathbf{U}_{n'}^{\dagger}\mathbf{E}_{n'}\mathbf{U}_{n'} - \tilde{\alpha}\mathbf{I}\right)^H\\ &+ |\beta|^2\mathbf{U}_{n'}^{\dagger}\mathbf{E}_{n'}^{*}\mathbf{U}_{n'}^{*}\mathbf{C}_{\boldsymbol{h}}\mathbf{U}_{n'}^{T}\mathbf{E}_{n'}\mathbf{U}_{n'}^{\dagger\,T} + 2\sigma_{\dot{w}}^2\left(\mathbf{U}_{n'}\mathbf{U}_{n'}^{H}\right)^{\dagger}\end{aligned}$$

and the CIR error variance is $\sigma^2_{\boldsymbol{\Delta h}} = \mathrm{Tr}\{\mathbf{C}_{\boldsymbol{\Delta h}}\}$. Using (17) and (32), we could approximate the CEE covariance matrix of the channel frequency coefficients (CFR) as $\mathbf{C}_{\boldsymbol{\Delta H}} = \tilde{\mathbf{F}}_{K\times L_g}\mathbf{C}_{\boldsymbol{\Delta h}}\tilde{\mathbf{F}}^H_{K\times L_g}$, where $\tilde{\mathbf{F}}$ is the Fourier matrix. Expanding ZFE into Taylor series up to first-order in the neighborhood of $\boldsymbol{\Delta}_H = \mathbf{0}$ gives

$$\mathbf{Z} = \tilde{\alpha}^{-1}\mathbf{H}^{-1} - \tilde{\alpha}^{-2}\mathbf{H}^{-1}\boldsymbol{\Delta}_H\mathbf{H}^{-1}. \qquad (18)$$

The error terms are identified from (15) and (18), and averaged over $\boldsymbol{a}$, $\boldsymbol{w}$ and $\boldsymbol{\Delta}_H$. In doing so, it is assumed that:

- Prototype filters are orthogonal i.e., $\Re\{\tilde{\mathbf{G}}_0\} = \mathbf{I}$ and $\Re\{\tilde{\mathbf{G}}_n\} = \mathbf{0},\ \forall\, n \neq 0$,
- Higher-order product terms have negligible statistical significance,
- Desired and image subcarriers are widely separated in frequency making $\mathcal{I}^{uc}_{n',m'}$ and $\mathcal{I}^{c}_{n',m'}$ independent, and
- CEE has negligible cross-correlation meaning that $\mathbf{C}_{\boldsymbol{\Delta H}}$ is nearly diagonal.

For notational brevity, we drop index $n'$ and obtain,

$$\sigma^2_{\mathrm{Img}} = \bar{\sigma}_s^2\sum_{n=-\tau+1}^{\tau}\mathrm{Tr}\Bigg\{\Re\Big\{|\tilde{\alpha}|^{-2}\boldsymbol{\Upsilon}_n^{\beta}\boldsymbol{\Upsilon}_n^{\beta^H}\left(\mathbf{H}^H\mathbf{H}\right)^{-1} + \tilde{\alpha}^{-2}\boldsymbol{\Upsilon}_n^{\beta}\boldsymbol{\Upsilon}_n^{\beta^T}\mathbf{H}^{-2}\Big\}\Bigg\} \qquad (19)$$

$$\sigma^2_{\mathrm{Est}} = \frac{\bar{\sigma}_s^2}{|\tilde{\alpha}|^4}\sum_{n=-\tau+1}^{\tau}\mathrm{Tr}\left\{\Re\left\{\boldsymbol{\Upsilon}_n^{\alpha}\boldsymbol{\Upsilon}_n^{\alpha^H}\right\}\left(\mathbf{H}^H\mathbf{H}\right)^{-2}\mathbf{C}_{\boldsymbol{\Delta H}}\right\} \qquad (20)$$

$$\sigma^2_{\mathrm{AWGN}} = \frac{\sigma_w^2}{2K}\mathrm{Tr}\Bigg\{\frac{\left(|\alpha|^2+|\beta|^2\right)}{\tilde{\alpha}^2}\left(\mathbf{H}\mathbf{H}^H\right)^{-1} + \Re\left\{\frac{\alpha\beta}{\tilde{\alpha}^2}\sum_{n=-\tau+1}^{\tau}\mathbf{F}_n^H\mathbf{F}_n^{*}\mathbf{H}^{-2}\right\}\Bigg\} \qquad (21)$$

which correspond to the distortion due to IQI, CEE and AWGN respectively, and $\bar{\sigma}_s^2 = \sigma_s^2/(4K)$. To obtain SINR degradation D, the error components identified in (19)-(21) are inserted in the SINR definition as follows:

$$\mathrm{SINR}_{\mathrm{Imp}} = \mathbb{E}_{\mathbf{H}}\left\{\frac{\sigma^2_{\mathrm{Des.}}}{\sigma^2_{\mathrm{ISI/ICI}} + \sigma^2_{\mathrm{Img}} + \sigma^2_{\mathrm{Est}} + \sigma^2_{\mathrm{AWGN}}}\right\} \qquad (22)$$

where $\sigma^2_{\mathrm{Des}} = 2\bar{\sigma}_s^2\left\|\Re\left\{\tilde{\alpha}^{-1}\mathbf{H}^{-1}\mathrm{diag}\left\{\boldsymbol{\Upsilon}_0^{\alpha}\right\}\right\}\right\|^2 = \sigma_s^2/2$ and $\sigma^2_{\mathrm{ISI/ICI}} = 2\bar{\sigma}_s^2\sum_n\left\|\Re\left\{\tilde{\alpha}^{-1}\mathbf{H}^{-1}\boldsymbol{\Upsilon}_n^{\alpha}\right\}\right\|^2 - \sigma^2_{\mathrm{Des}}$. $\mathrm{SINR}_{\mathrm{Ideal}}$ is (22) in the absence of IQI and CFO, and with perfect CSI. Let $\sigma^2_{\mathrm{I}} = \sigma^2_{\mathrm{ISI/ICI}} + \sigma^2_{\mathrm{Img}} + \sigma^2_{\mathrm{Est}}$, $\sigma^2_{\mathrm{N}} = \sigma^2_{\mathrm{AWGN}} + \sigma^2_{\mathrm{I}}$ and $\sigma^2_{\mathrm{AWGN}} \approx \sigma_w^2/2$. Then, it is evident that at high SNR, $\mathrm{D} \to \infty$, as $\sigma^2_{\mathrm{I}} \to \sigma^2_{\mathrm{N}}$. Overall, the effect of receiver imperfections is to push $\mathrm{SINR}_{\mathrm{Imp}}$ asymptotically towards a floor and hence, an unbounded increase in degradation results.

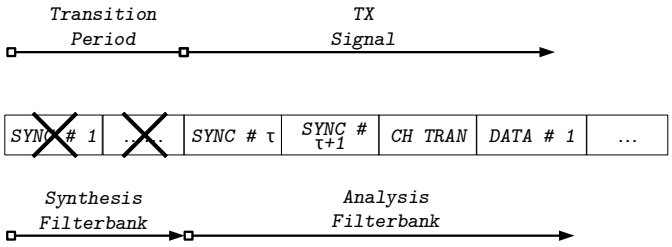


Fig. 1: The proposed preamble structure with preamble shortening to reduce training overhead for OFDM/OQAM frame transmission.

## IV. ML Estimation Technique

In order to enhance the robustness of the OFDM/OQAM system to non-idealities, an estimation procedure for the IQI and CFO mitigation is briefly described in this section.[2]

### A. Joint IQI and CFO Estimation:

For synchronization and channel estimation purposes, the frame structure in most of the current wireless communication standards contain a set of training signals. We here assume that identical pseudo-noise sequences are transmitted in the beginning of the frame. If we allow a delay of $L/2$ samples, that is sufficient to fully load the prototype filter, it is obvious from (1) [8] that $\boldsymbol{u}_{\tau} = -\jmath\boldsymbol{u}_{\tau+1}$. However, the redundant SYNC symbol blocks lead to high training overhead. In this paper, we propose a truncated preamble design as shown in Fig. 1 which is suitable for time-domain parameter estimation and establishes fairness w.r.t to the conventional OFDM/QAM systems. A possible issue is the prototype filter mismatch for the first few data symbol blocks. Nevertheless, if $\tau$ is small or pulse $g(k)$ decays sufficiently, this truncation for $n < \tau$ does not induce any distortion.

Next step is to find a metric suitable for the estimation of IQI and CFO, ignoring CIR. This can be achieved by writing $\boldsymbol{r}_{\tau+1}$ as a function of $\boldsymbol{r}_{\tau} = [r(\tau M), r(\tau M+1), \ldots, r((\tau+1)M-1)]^T$ and using the fact that corresponding samples in the repetitive sequence suffer fixed relative phase rotation[3] of $\overline{\phi} = \pi\overline{\Delta f}$ [10]. Substituting the noiseless faded signal $\boldsymbol{v}_{\tau}$ in the expression for $\boldsymbol{r}_{\tau+1}$, we get

$$\boldsymbol{r}_{\tau+1} = \eta\boldsymbol{r}_{\tau} + \chi\boldsymbol{r}_{\tau}^{*} + \tilde{\boldsymbol{w}}_{\tau:\tau+1} \qquad (23)$$

where the effective noise term $\tilde{\boldsymbol{w}}_{\tau:\tau+1}$ is complex Gaussian with zero-mean and variance $\sigma^2_{\tilde{w}} = \left(1+(1+\varepsilon)^2\right)\sigma_w^2$, $\eta = \left(\exp\left(-\jmath\overline{\phi}\right) - |\gamma|^2\exp\left(\jmath\overline{\phi}\right)\right)/\left(1-|\gamma|^2\right)$, $\chi = \jmath 2\gamma\sin(\overline{\phi})/\left(1-|\gamma|^2\right)$ and $\gamma = \beta/\alpha^*$ is the IQI decoupling variable. In practice, IQI is usually small i.e, $|\gamma| \approx 0$ and the noise variance $\sigma^2_{\tilde{w}}$ is nearly independent of the estimation parameters. Therefore, the negative log-likelihood function can be written as

$$\begin{aligned}\Lambda\left(\gamma,\overline{\phi}\right) \;\widetilde{\propto}\; &\boldsymbol{r}_{\tau+1}^H\boldsymbol{r}_{\tau+1} + \left(|\eta|^2+|\chi|^2\right)\boldsymbol{r}_{\tau}^H\boldsymbol{r}_{\tau}\\ &- 2\Re\left\{\eta\boldsymbol{r}_{\tau+1}^H\boldsymbol{r}_{\tau} + \chi^*\boldsymbol{r}_{\tau+1}^T\boldsymbol{r}_{\tau} - \eta\chi^*\boldsymbol{r}_{\tau}^T\boldsymbol{r}_{\tau}\right\}. \qquad (24)\end{aligned}$$

The joint maximum-likelihood (ML) estimator is obtained by first searching for $\gamma$ that minimizes the log-likelihood

[2]Opposed to frequency-domain parameter estimation [14], modulated observation (5) usage is preferable due to the intricate nature of the estimation and correction problems, when operating directly on demodulated signal $\boldsymbol{y}_{n'}$.

[3]The constant phase shift of $\pi/2$ in $\boldsymbol{u}_{\tau+1}$ is disregarded for exposition.

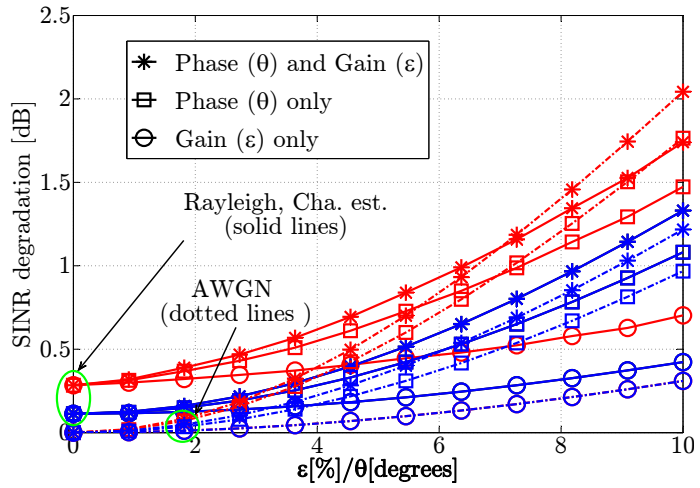


Fig. 2: SINR degradation vs the IQI parameters for **OFDM/OQAM (red)** and **CP-OFDM/QAM (blue)**: SNR= 15 dB.

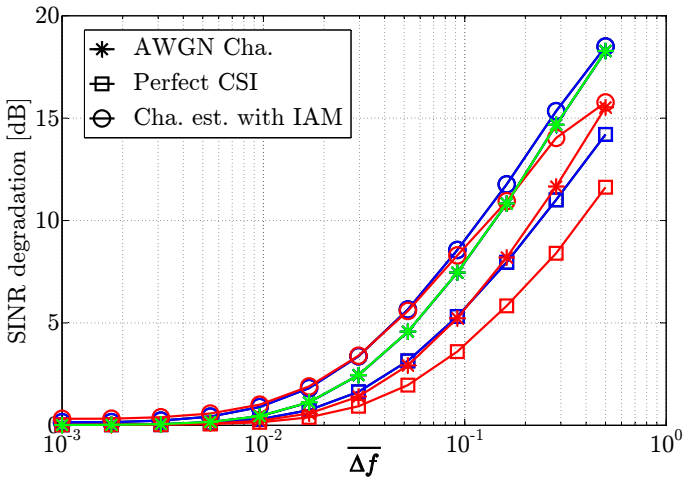


Fig. 3: SINR degradation vs the normalized CFO for **OFDM/OQAM (red)**, **OFDM/QAM (green)** and **CP-OFDM/QAM (blue)**: SNR= 15 dB.

function for a fixed $\overline{\phi}$. Neglecting higher-order terms of (24), taking derivative w.r.t. $\gamma^*$, and setting to zero, the ML estimate is

$$\widehat{\gamma} = \frac{\jmath \sin(\overline{\phi}) \left( e^{-\jmath\overline{\phi}} \boldsymbol{r}_\tau^T \boldsymbol{r}_\tau - \boldsymbol{r}_{\tau+1}^T \boldsymbol{r}_\tau \right)}{\Re\left\{ e^{\jmath\overline{\phi}} \boldsymbol{r}_{\tau+1}^H \boldsymbol{r}_\tau \right\} + \left(1 - 2\cos\left(2\overline{\phi}\right)\right) \boldsymbol{r}_\tau^H \boldsymbol{r}_\tau}. \tag{25}$$

The second term in (24) depends weakly on $\overline{\phi}$ and the last term inside real operator can be neglected. Under these assumptions, the function $\Lambda\left(\gamma, \overline{\phi}\right)$ in (24) achieves its minimum at

$$\widehat{\Delta w T_s} = \frac{1}{M} \angle \left( \left( \boldsymbol{r}_{\tau+1} - \widehat{\gamma} \boldsymbol{r}_{\tau+1}^* \right)^H \left( \boldsymbol{r}_\tau - \widehat{\gamma} \boldsymbol{r}_\tau^* \right) \right) \tag{26}$$

where $\angle(\cdot)$ derives the phase of the argument. Basically (26) is similar to the classical CFO estimator [8] using IQI corrected signal as observation. Note that there is a need to restrict the frequency error range to $|\Delta w T_s| \leq \pi/K$ for the CFO estimator in (26).

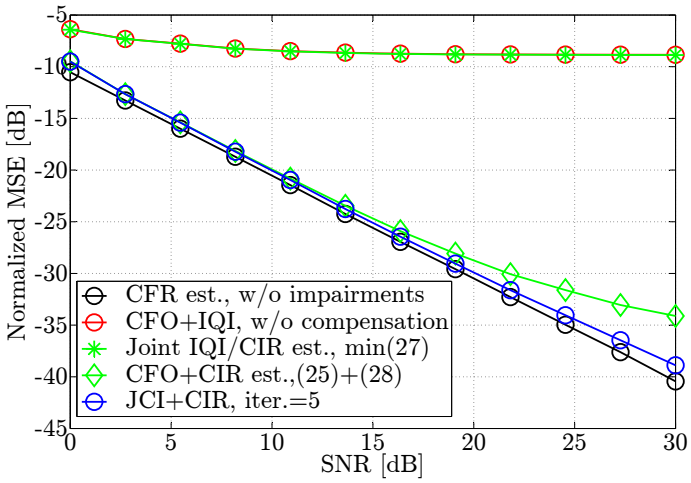


Fig. 4: MSE vs SNR performance of the OFDM/OQAM channel estimator; CFO: $\overline{\Delta f} \in \mathcal{U}\{0, 1/8\}$ and IQI: $\varepsilon/\theta \in \mathcal{U}\{0, 10\}\%/\text{Degrees}$.

### *B. Channel Estimation:*

If the CIR is finite length and IQI/CFO parameters are known, it is more efficient to estimate the channel in time-domain. However, redundancy exploited in (24) is not suitable for CIR estimation. Absence of cyclic prefix in a typical OFDM/OQAM system requires a delay of $L_g$ samples in the system model, so that

$$\tilde{\boldsymbol{r}}_{n'} = \alpha \mathbf{E}_{n'} \mathbf{U}_{n'} \boldsymbol{h} + \beta \mathbf{E}_{n'}^* \mathbf{U}_{n'}^* \boldsymbol{h}^* + \tilde{\boldsymbol{w}}_{n'} \tag{27}$$

where $\tilde{\boldsymbol{r}}_{n'} = [r(L_g + n'M), r(L_g + n'M + 1), \ldots, r(L_g + (n'+1)M - 1)]^T$. The ML-estimate of $\boldsymbol{h}$ is obtained by optimizing the following log-likelihood function for a given $\widehat{\gamma}$ and $\widehat{\mathbf{E}}_{n'}$:

$$\Lambda\left(\boldsymbol{h}\right) \propto \left\| \tilde{\boldsymbol{r}}_{n'} - \widehat{\gamma} \tilde{\boldsymbol{r}}_{n'}^* - \widehat{\mathbf{E}}_{n'} \mathbf{U}_{n'} \boldsymbol{h} \right\|^2 \tag{28}$$

whose minimum is achieved at

$$\widehat{\boldsymbol{h}} = \mathbf{U}_{n'}^{\dagger} \widehat{\mathbf{E}}_{n'}^* \left( \tilde{\boldsymbol{r}}_{n'} - \widehat{\gamma} \tilde{\boldsymbol{r}}_{n'}^* \right). \tag{29}$$

Note that after IQI correction in (29), the scaling remnant $\bar{\alpha} = \alpha(1 - |\gamma|^2)$ becomes a part of the channel estimate and will be canceled while performing ZFE on the compensated symbols.

## V. Numerical Results

Computer simulations were carried out to verify the performance with the number of subcarriers $K = 256$ and an overlapping factor of $\tau = 4$. The results were averaged over 1000 Monte-Carlo simulations for each SNR value and a fixed data symbol position inside an OFDM frame (first data symbol block). The FIR channels were simulated with complex Gaussian taps having exponential power delay profile $\sigma_l^2 = c \exp(-l/\sigma_{rms})$, $\forall\ l \in [0\ L_g - 1]$, $\sigma_{rms} = 4$, $L_g = 5$ and $c$ such that $\sum_l \sigma_l^2 = 1$. The prototype filter is based on extended Gaussian pulses with $\tau_0 \nu_0 = 1/2$ and $\lambda = 2$ [6].

Fig. 2 and Fig. 3 depict the degradation in SINR when the receiver front-end suffers from the IQI and CFO distortion, respectively. We can notice that while OFDM/OQAM exhibits more robustness against CFO distortion as compared to CP-OFDM/QAM, it is at the same time more sensitive to IQI problem in DCRs. The phase imbalance in Fig. 2 causes more degradation in OFDM/OQAM than OFDM/QAM over

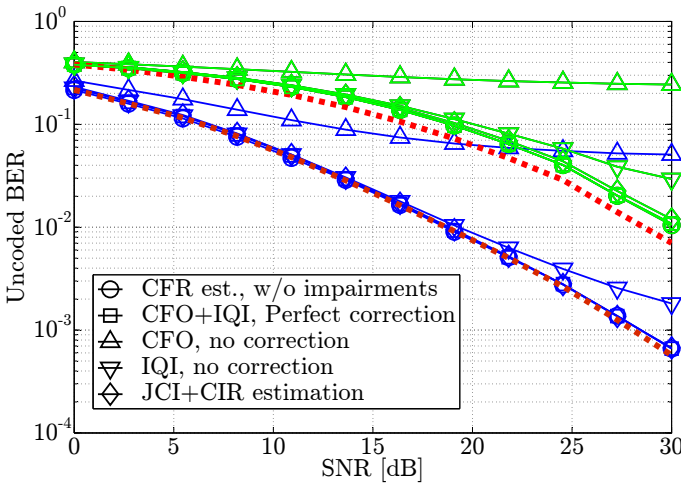


Fig. 5: BER vs SNR performance of the OFDM/OQAM system with **QPSK (blue)**, **64-QAM (green)** and **ideal CP-OFDM/QAM with channel estimation (red dotted)**; CFO: $\overline{\Delta f} \in \mathcal{U}\{0, 1/8\}$ and IQI: $\varepsilon/\theta \in \mathcal{U}\{0, 10\}\%/\text{Degrees}$.

AWGN channels whereas the impact of gain imbalance is equivalent, validating the findings of Section II-B. Moreover, CEE in OFDM/OQAM system causes an additional degradation of around 0.3 dB. In case of CFO, spectral confinement of OFDM/OQAM provides a peak improvement of about 2.5 dB, both for the perfect and estimated CSI. Interestingly, the degradation comes out relatively lower for fading channels, which is plausible as ISI/ICI composition is affected by fading frequency-selectivity. Nevertheless, the absolute SINR (not shown) was still superior for AWGN channels to begin with.

Fig. 4 demonstrates the error performance of the CFR estimator (29), with normalized MSE $\triangleq \mathbb{E}\{\|\bar{\alpha}\mathbf{H} - \hat{\mathbf{H}}\|^2/\|\bar{\alpha}\mathbf{H}\|^2\}$, in conjunction with iterative joint CFO and IQI estimator (JCI). CFO and IQI are uniformly distributed in the specified range. The results show that the presented technique provides the channel estimates within 2 dB performance loss with impaired receivers, when compared to the classical CFR estimator [14] with ideal RF front-end.

In Fig. 5 we compare the bit-error-rate (BER) performance of the OFDM/OQAM system with imperfections. It shows that the compensation scheme was able to remove nearly all interference in QPSK modulated system and has error performance in the vicinity of the ideal system. Preamble truncation, that is expected to effect the first data symbol block (due to overlapping factor of $\tau = 4$), seems to have no impact. For 64-QAM, the approximations used in (32) and one-tap ZFE have overwhelming influence. Moreover, the residual interference after compensation causes a slight performance degradation.

## VI. Conclusion

We considered OFDM/OQAM system with non-ideal receivers and imperfect CSI. While a comparative robustness to CFO was widely anticipated, OFDM/OQAM system is shown to be more sensitive to IQI effects. Degradation suffered as a consequence of the imperfect receiver processing was quantified in terms of the SINR loss. To alleviate the IQI/CFO distortion and obtain reliable channel estimates for the coherent reception, a joint estimation algorithm was discussed. We found that with the compensation scheme in place and in a quasi-static Rayleigh-fading scenario, the presence of IQI and CFO incurs at most 1 dB loss in the error performance.

## Appendix A
## I/O Relationship for Time-dispersive Channels

Let us ignore RF distortion in (6) and impose the constraint that the modulation pulse $g(n)$ is real-valued and symmetric. This ensures that the Fourier transform of the autocorrelation function is real (see (34)). Then, $y_{n',m'}$ can be rewritten as

$$y^0_{n',m'} = \sum_{m,n,k,l} \zeta^*_{n',m'}(k) h(l) \zeta_{n,m}(k-l) a_{n,m} + w_{n',m'} \quad (30)$$

$$\overset{(a)}{=} \frac{1}{K} \sum_{m,n,l,q} e^{\jmath \frac{2\pi}{K} l \left(q - \frac{m+m'}{2}\right)} e^{\jmath \tilde{\theta}^{n,m}_{n',m'}(l')} \times H(q) A_g(\Delta n - l', \Delta m) a_{n,m} + w_{n',m'} \quad (31)$$

$$\overset{(b)}{\approx} H(m') A_g(0,0) a_{n',m'} + \sum_{(n,m)\notin(n',m')} e^{\jmath \tilde{\theta}_{\Delta n, \Delta m}} \times H\left(\frac{m+m'}{2}\right) A_g(\Delta n, \Delta m) a_{n,m} + w_{n',m'} \quad (32)$$

where $w_{n',m'} = \langle w, \zeta^*_{n',m'} \rangle$ and $H\big((m+m')/2\big)$ is the Fourier transform of $h(t)$ at the intermediate frequency $(m+m')/(2T)$, approximated as $H(m)$ in [14]. The step $(a)$ can be understood from the cross-correlation between $\zeta_{n,m}(k)$ and $\zeta_{n',m'}(k)$ as

$$\sum_k \zeta^*_{n',m'}(k) \zeta_{n,m}(k-l) = e^{\jmath(\varphi_{n,m} - \varphi_{n',m'})} e^{-\jmath \frac{2\pi}{K} lm} \times \sum_k e^{\jmath \frac{2\pi}{K} k(m-m')} g\left(k - n'M\right) g\left(k - l - nM\right) \quad (33)$$

$$\overset{(c)}{=} e^{\jmath \tilde{\theta}^{n,m}_{n',m'}(l')} \sum_{k'} e^{-\jmath \frac{2\pi}{K} k' \Delta m} \times g\left(k' - \frac{\Delta nM - l}{2}\right) g\left(k' + \frac{\Delta nM - l}{2}\right) \quad (34)$$

$$= e^{\jmath \tilde{\theta}^{n,m}_{n',m'}(l')} A_g(\Delta n - l', \Delta m) \quad (35)$$

$$\overset{(d)}{\approx} \begin{cases} \pm A_g(\Delta n, \Delta m) & (\Delta n, \Delta m) \in \Omega' \\ \pm \jmath A_g(\Delta n, \Delta m) & \text{Otherwise} \end{cases} \quad (36)$$

where $\Delta n = n' - n$, $\Delta m = m' - m$, $\Omega' = \{(\Delta n, \Delta m) | (\Delta n)_2 = (\Delta m)_2 = 0\}$, $l' = l/M$, $\tilde{\theta}^{n,m}_{n',m'}(l') = (\pi/2)(n'm' - nm + n'm - nm' - \Delta m - \Delta n - l'(m+m'))$ and $\tilde{\theta}_{\Delta n, \Delta m} = \tilde{\theta}^{n,m}_{n',m'}(0)$. We made the substitution $k = k' + (l + (n+n')M)/2$ in step $(c)$ and neglected $\varrho$. If the channel is deterministically underspread i.e., small $L_g$ and $\zeta_{n,m}(k)$ is locally smooth over span $L_g$ and has sufficient decay overall, we can drop summation over $\{l, q\}$ in (31), since $(1/K)\sum_{m,l} H(m) \exp\left(\jmath 2\pi l(m-n)/K\right) = H(n)$ leading to step $(b)$. Note that $(d)$ converges to equality when $K \to \infty$.

## References


[1] T. Strohmer and S. Beaver, "Optimal OFDM design for time-frequency dispersive channels," *IEEE Trans. Commun.*, vol. 51, no. 7, Jul. 2003.

[2] H. Bolcskei, "Blind estimation of symbol timing and carrier frequency offset in wireless OFDM systems," *IEEE Trans. Commun.*, vol. 49, no. 6, pp. 988–999, Jun. 2001.

[3] W. Kozek and A. Molisch, "Nonorthogonal pulseshapes for multicarrier communications in doubly dispersive channels," *IEEE J. Sel. Areas Commun.*, vol. 16, no. 8, pp. 1579–1589, Oct. 1998.

[4] S. Das and P. Schniter, "Max-SINR ISI/ICI-shaping multicarrier communication over the doubly dispersive channel," *IEEE Trans. Signal Process.*, vol. 55, no. 12, pp. 5782–5795, Dec. 2007.

[5] "Physical layer aspects for evolved universal terrestrial radio access (UTRA)," *3GPP TR 25.814 V7.1.0 (2006-09)*.

[6] P. Siohan, C. Siclet, and N. Lacaille, "Analysis and design of OFDM/OQAM systems based on filterbank theory," *IEEE Trans. Signal Process.*, vol. 50, no. 5, pp. 1170–1183, May 2002.

[7] P. Remvik, N. Holte, and A. Vahlin, "Fading and carrier frequency offset robustness for different pulse shaping filters in OFDM," in *IEEE VTC, 1998*, vol. 2, 1998, pp. 777–781.

[8] T. Fusco, A. Petrella, and M. Tanda, "Data-aided symbol timing and CFO synchronization for filter bank multicarrier systems," *IEEE Trans. Wireless Commun.*, vol. 8, no. 5, pp. 2705–2715, May 2009.

[9] H. Sourck and et al., "Effect of carrier frequency offset on offset QAM multicarrier filter bank systems over frequency-selective channels," in *IEEE WCNC, 2010*, 2010, pp. 1–6.

[10] F. Horlin and et al., "Low-complexity EM-based joint CFO and IQ imbalance acquisition," in *ICC, 2007.*, pp. 2871–2876.

[11] Y.-H. Chung and S.-M. Phoong, "Joint estimation of I/Q imbalance, CFO and channel response for MIMO OFDM systems," *IEEE Trans. Commun.*, vol. 58, no. 5, pp. 1485–1492, 2010.

[12] H. Lin and P. Siohan, "A new transceiver system for the OFDM/OQAM modulation with cyclic prefix," in *IEEE PIMRC, 2008.*, 2008, pp. 1–5.

[13] ——, "Robust channel estimation for OFDM/OQAM," *IEEE Commun. Lett.*, vol. 13, no. 10, pp. 724–726, Oct. 2009.

[14] D. Katselis and et al., "Preamble-based channel estimation for CP-OFDM and OFDM/OQAM systems: A comparative study," *IEEE Trans. Signal Process.*, vol. 58, no. 5, pp. 2911–2916, May 2010.